

EFFECT OF HEAT TREATMENT OF 316L STAINLESS STEEL PRODUCED BY SELECTIVE LASER MELTING (SLM)

M. L. Montero Sistiaga*, S. Nardone[†], C. Hautfenne[†] and J. Van Humbeeck *

* KU Leuven, Department of Materials Engineering, Heverlee B-3001, Belgium.

[†]Engie Lab, Linkebeek B-1630, Belgium

Abstract

Selective Laser Melting (SLM) shows a big potential within additive manufacturing of metals. The competitive mechanical properties compared to conventional processes as well as the geometry freedom are the main advantages of SLM. 316L stainless steel has been investigated in previous works regarding microstructure and mechanical properties. However, the influence of heat treatments has not been fully reported yet. This work studies the influence of different heat treatments applied to 316L stainless steel produced by SLM. The microstructure evolution was investigated for different conditions. Tensile, Charpy and hardness tests were performed on the as built and heat treated samples.

Keywords: Selective Laser Melting, Additive Manufacturing, 316L, heat treatment

Introduction

Selective Laser Melting (SLM) is an Additive Manufacturing process which locally melts a metallic powder bed using a highly focus laser beam. The high cooling rates result in a unique microstructure, but may introduce residual stresses making the material susceptible to distortion [1]. The high flexibility in design, low material waste and fast production of near-net-shape parts are the main advantages compared to conventional processing routes.

316L stainless steel has been widely investigated for SLM. High relative densities and competing mechanical properties have been achieved. The optimization process for 316L has been reported by many authors [2], [3]. The work of Yasa et al. showed that re-melting results in an increase of density and surface quality. After SLM a sub-micron cellular-dendritic solidification microstructure is observed caused by the high thermal gradients during cooling. These cells are oriented more or less towards the heat gradient inside the melt pool [4], [5]. Referring to the mechanical properties, the yield strength of SLM processed 316L parts appear to be much higher than wrought 316L, and a large difference in elongation is found between horizontal and vertical built samples [6], [7]. Due to the presence of large thermal gradients and the local melting and solidification processes during SLM, microstructural and mechanical

anisotropy are inherent to happen [6], [7]. The fatigue properties of SLM processed 316L parts have been investigated[8], [9].

This work aims at better understanding the effect of the heat treatments on the microstructural and mechanical behavior of 316L parts produced by SLM. Tensile and Charpy test were performed to investigate the evolution in mechanical properties after applying different heat treatments.

Materials and methods

The material used in this study was 316L stainless steel provided by SLM solutions GmbH and with powder particles sizes ranging from 10 to 45 μm . The 316L powder composition is shown in Table 1 as defined in ASTM B243. The powder morphology is shown in Figure 1. The particles show mainly spherical shaped granules with some smaller satellite particles attached.

Table 1. Chemical composition in weight % of 316L powder.

Weight [%]	Fe	Cr	Ni	Mo	Mn	Si	P	S	C	Density [g/cm^3]
316L powder	Bal.	16.8	10.4	2.1	1.11	0.56	0.03	0.011	0.01	7.985

The SLM 280 selective laser melting machine was used for the production of the 316L samples. The SLM instrument is equipped with 400W fiber laser. All the parts were built under argon atmosphere to avoid oxidation and using a pre-heating temperature of 100°C. A relative density of around 99.3% was achieved for all samples measured by Archimedes method using a theoretical density of 7.985 g cm^{-3} .

For microstructural observations the samples were grinded, polished and chemically etched during 30s using 10% oxalic acid dissolved in H_2O . The samples were examined using an Axioskop 40Pol/40 A Pol optical microscope (LOM) and Philips XL30FEG Scanning Electron Microscope (SEM). The crystallographic orientation was studied using electron backscattered diffraction (EBSD) using a Philips XL30 SEM equipped with a TSL orientation imaging microscope system.

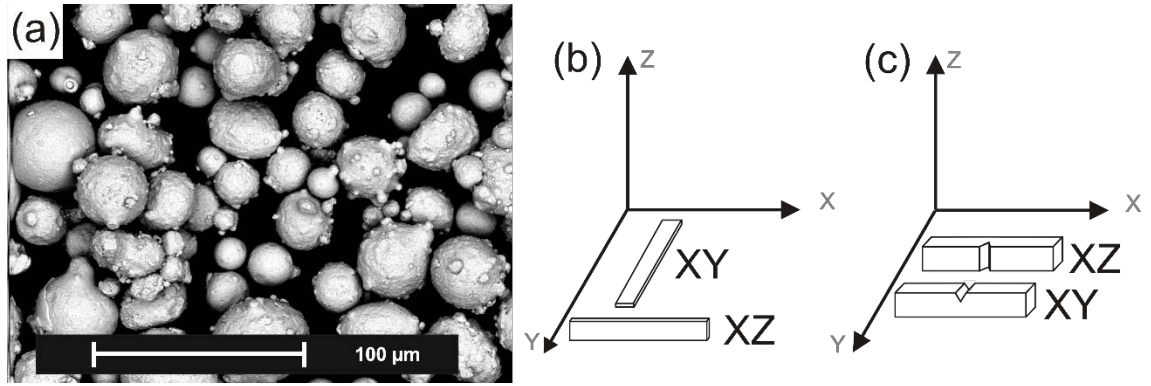


Figure 1. 316L stainless steel powder morphology (a). Part positioning for the tensile (b) and Charpy (c) test.

Rectangular tensile test specimens were built in two directions XY and XZ (see Figure 1b). The samples were tested in an Instron 4505 at a cross head velocity of 1 mm min^{-1} according to ASTM E 8M. Rectangular bars with size $12 \times 12 \times 56 \text{ mm}^3$ were horizontally built and later machined for the Charpy V-notch test according to ASTM E23. Two different directions were tested with the notch in XY and XZ direction (see Figure 1c). The Vickers hardness tester FV-700 was used for measuring the Vickers hardness with 0.5 kg load for 15s with five repetitions per sample.

Heat treatments were performed using a vertical tube furnace under argon atmosphere and with a heating rate of $10^\circ\text{C min}^{-1}$. The different treatments are depicted in Table 2. HT1 and HT2 apply air cooling and HT3 applies water quenching.

Table 2. Heat treatments applied to the 316L tensile and Charpy samples.

Heat treated (HT)	HT cycle
HT1	600°C 2h, air cooling
HT2	950°C 2h, air cooling
HT3	1095°C 2h, water cooling

Results and discussion

1. Microstructure evolution after heat treatments

Figure 2 shows the side view microstructures for the as built (AB) and heat treated samples by SEM. For the AB and HT1 (Figure 2a-b) condition, melt pool boundaries are visible. The grains grow across these melt pools parallel to the building directions, in the direction of the heat gradient. Inside the grains, a clear cellular dendritic microstructure is observed, with cell sizes ranging between 0.5 and $1 \mu\text{m}$. The microstructures observed by SEM for samples HT2

(Figure 2c) and HT3 (Figure2d) present no cellular dendrites inside the grains. The melt pool boundaries are almost dissolved and only the grains are observed. After etching, some homogeneously distributed round pits appear inside the grains for HT2 and HT3 at higher magnifications. Although no substructure can be observed for HT2 and HT3 (e.g. cellular dendrites) small chemical variations within the grain could act as initiation sites of pitting. The difference in pit size between HT2 and HT3 can be related to the etching time variance

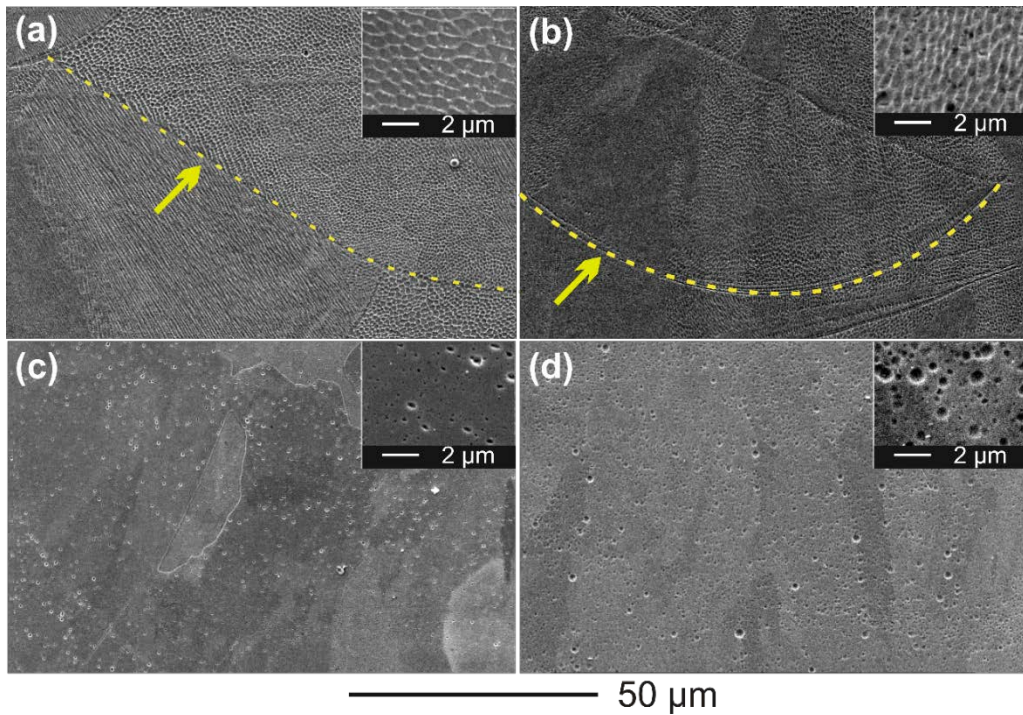


Figure 2 Secondary electron image of the side view of 316L stainless steel produced by SLM. (a) As built (AB), (b) HT1, (c) HT2 and (d) HT3 conditions. The arrows are indicating the melt pool border, present for AB and HT1 samples.

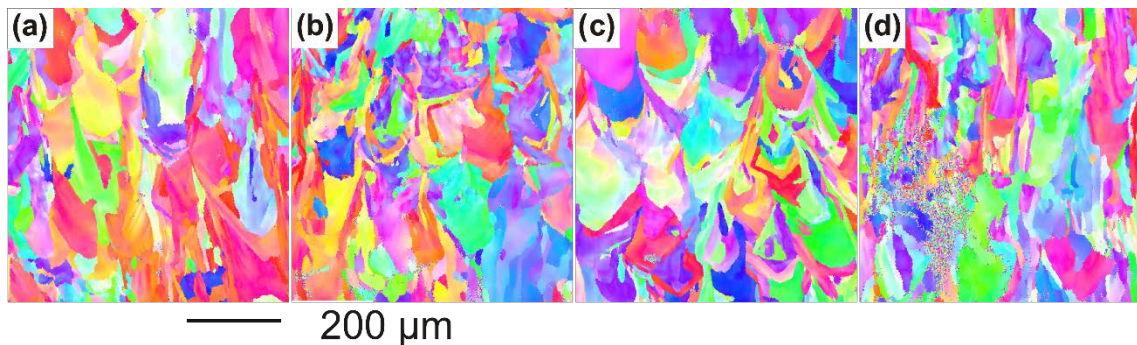


Figure 3. EBSD orientation maps of samples AB (a), HT1 (b), HT2 (c) and HT3 (d), plane parallel to the building direction.

Figure 3 depicts the EBSD image of the side view for the AB sample. The results are in consistence with the SEM observations. Columnar grains grow parallel to the building direction

with longitudinal size around 100 μm . The EBSD results conducted for HT1, HT2 and HT3 shows no difference in grain size in comparison with the AB samples. Thus the heat treatments applied to the as built samples do not show grain enlargement. All the samples show grains directed parallel to the building.

2. Mechanical Properties

Vickers micro-hardness measurements are presented in Table 3. The hardness for conventionally produced 316L is also listed as a reference. The experimental results obtained for the SLM processed parts in AB and heat treated condition are well above the requirements. For the AB condition, a hardness of 245 ± 25 HV was measured. The AB hardness is in accordance with the values found in literature, with hardness values around 235HV [4], [6]. HT1, which applies only a heat treatment at 600°C , increases the AB hardness up to 271 ± 25 HV. HT2 and HT3 creates lower values than AB and HT1.

Table 3. Vickers micro hardness measurements of the side view of the SLM processed samples.

Condition	AB	HT1	HT2	HT3	Ref. [10]
Vickers hardness [HV]	245 ± 21	271 ± 25	215 ± 14	212 ± 20	155

The tensile test and Charpy-V test were performed on the as built and heat treated samples. The results are shown in Figure 4. EM10216-5:2013 standard is also listed as reference for the elongation, yield tensile strength (YTS) and ultimate tensile strength (UTS) values. All samples exhibit a much higher YTS compared to the standard. For the UTS all values lie within the limitations of the standard. On the other hand, varying elongation values with wide standard deviations are observed. The porosities or impurities found after the SLM process can deteriorate the ductility values, but they do not affect other properties such as UTS. Nevertheless, most of the samples lie close to the EN 10216-5:2013 standard.

AB and HT1 samples exhibit a higher yield and ultimate strength compared to HT2 and HT3. According to the grain boundary strengthening the grain size influences the yield strength in 316L[4]. HT2 and HT3 present a grain size similar to the AB and HT1, but no cellular dendritic substructure (see Figure 2). This suggests that the high strength obtained by AB and HT1 is attributed to the presence of a cellular dendritic substructure. The dislocations could accumulate at boundaries of the cells, acting as a strengthening sites [4]. This also can explain the high hardness (see Table 3) obtained for samples AB and HT1 compared to HT2 and HT3.

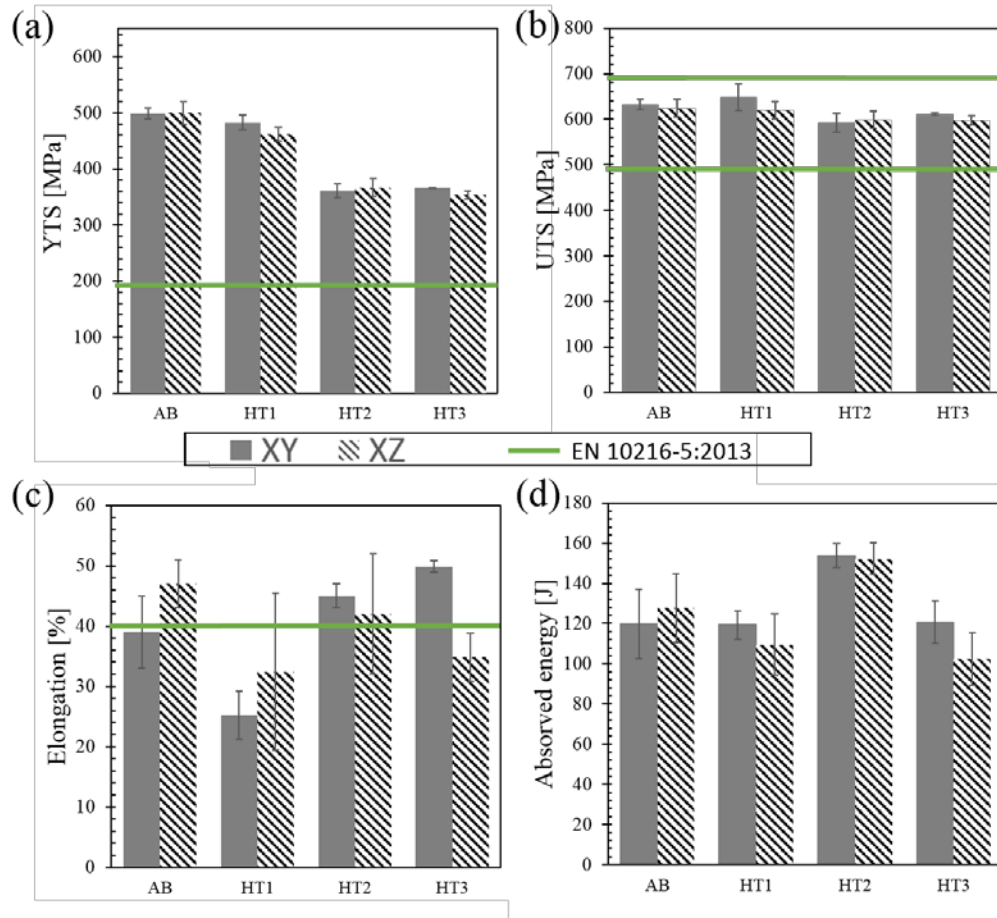


Figure 4 Mechanical properties of 316L in as built (AB) and heat treated conditions (HT1, HT2, HT3) and compared with EN 10216-5:2013 standard.

Charpy test results are presented in Figure 4d for the AB and HT1-3 samples. HT2 shows the highest absorbed energy with 154 ± 6 J for XY direction and 152 ± 8 J for XZ direction. HT1 and HT3 samples show similar toughness compared to the AB condition. For HT2 the reduction of tensile strength maintaining the elongations observed in the tensile values results in an improved toughness compared to the AB condition. On the other hand, HT2 and HT3 show similar microstructure as seen in Figure 2, but significantly different absorbed energies. HT3 is subjected to a dwell temperature higher than HT2 during the same time (2h) and the sample is subsequently water quenched. The reduced toughness obtained for HT3 could be accounted for the effect of water cooling, which could induce stresses to the material. However, the influence of air cooling and water quenching after the same heat treatment should be further investigated. All the values obtained by the Charpy test (absorbed energy) obtained in this work show higher values than the ones found in literature for SLM of 316L.

The fracture surfaces of the Charpy samples were analyzed in order to understand the differences in mechanical properties after the different heat treatments. Figure 5 displays the fracture surfaces for all the samples. In Figure 5e, the very ductile fracture can be observed, visible for all the condition. At a closer look with the SEM, the classic dimple structure can be observed. No non-molten particles can be observed for all samples, proving the good consolidation of the parts. Sample HT3 (Figure 5d) shows wider and shallower dimple structures, which could explain the lower impact toughness compared to HT2. For samples AB, HT1 and HT3, the dimple sizes are comparable to the one of the cells. The observed dimples show a size between 0.5 and 1 μm , even for HT3 where no cellular dendrites were observed.

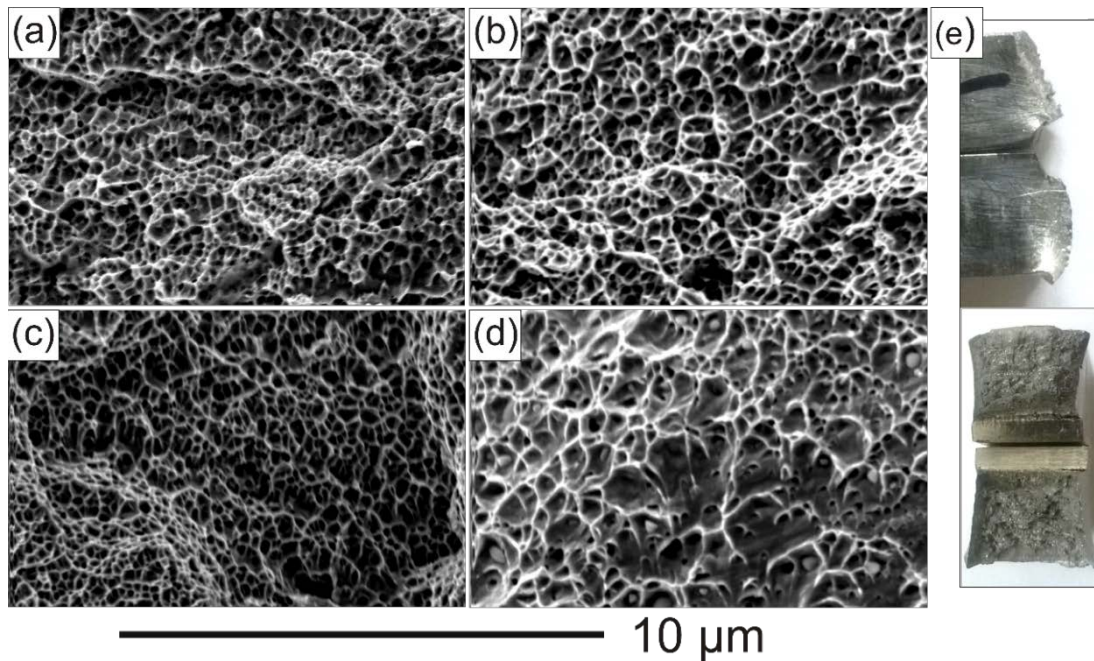


Figure 5. Fracture surfaces of SLM processed 316L after Charpy test using scanning electron microscope for (a) as built, (b) HT1, (c) HT2 and (d) HT3 samples. Optical image of side and front view of the surface fracture, showing a ductile mode (e).

Conclusions

- 316L stainless steel processed by SLM results in much higher yield and ultimate strength, while keeping the high elongation of the wrought material.
- Heat treatments above 950°C show no grain enlargement compared to the as built condition, but the cellular dendritic structure is completely dissolved. This results in lower hardness and yield strength compared to the as built condition.
- HT2 (heat treatment at 950°C) results in a promising heat treatment to be applied on 316L produced by SLM. HT2 reduces the yield and ultimate strength of the as built samples but

still resulting in higher values than requirement from EM10216-5:2013 standard (190MPa). In addition, the absorbed energy, measured by the Charpy test, is significantly increased compared to the as build condition.

- Inclusions or formation of oxides can reduce and exhibit a wide spread in the elongation values of the SLM processed 316L.

Acknowledgments

This research was supported by the ENGIE Research and Technology Division. The authors acknowledge ENGIE Research and Technology Division for the use of the SLM280HL machine

References

- [1] P. Mercelis and J. Kruth, "Residual stresses in selective laser sintering and selective laser melting," *Rapid Prototyp. J.*, vol. 12, no. 5, pp. 254–265, Oct. 2006.
- [2] I. Yadroitsev, A. Gusarov, I. Yadroitsava, and I. Smurov, "Single track formation in selective laser melting of metal powders," *J. Mater. Process. Technol.*, vol. 210, no. 12, pp. 1624–1631, Sep. 2010.
- [3] A. B. Spierings and G. Levy, "Comparison of density of stainless steel 316L parts produced with selective laser melting using different powder grades," in *SFF symposium*, 2009.
- [4] Y. Zhong, L. Liu, S. Wikman, D. Cui, and Z. Shen, "Intragranular cellular segregation network structure strengthening 316L stainless steel prepared by selective laser melting," *J. Nucl. Mater.*, vol. 470, pp. 170–178, Mar. 2016.
- [5] E. Yasa and J.-P. Kruth, "Microstructural investigation of Selective Laser Melting 316L stainless steel parts exposed to laser re-melting," *Procedia Eng.*, vol. 19, pp. 389–395, 2011.
- [6] I. Tolosa, F. Garciandía, F. Zubiri, F. Zapirain, and A. Esnaola, "Study of mechanical properties of AISI 316 stainless steel processed by selective laser melting", following different manufacturing strategies," *Int. J. Adv. Manuf. Technol.*, vol. 51, no. 5, pp. 639–647, 2010.
- [7] G. Witt and J. T. ; Sehart, "Static strength analysis of beam melted parts dependent on various influences," in *SFF symposium*, 2010.
- [8] A. B. Spierings, T. L. Starr, and K. Wegener, "Fatigue performance of additive manufactured metallic parts," *Rapid Prototyp. J.*, vol. 19, no. 2, pp. 88–94, 2013.
- [9] A. Riemer, S. Leuders, M. Thöne, H. A. Richard, T. Tröster, and T. Niendorf, "On the fatigue crack growth behavior in 316L stainless steel manufactured by selective laser melting," *Eng. Fract. Mech.*, vol. 120, pp. 15–25, Apr. 2014.
- [10] J. W. Bray, "Materials Park," in *ASM Handbook, Materials Park*, OH: ASM International, 1990.